

Growth of GaAs_{1-x}Bi_x layers by molecular-beam epitaxy

© B.R. Semyagin¹, A.V. Kolesnikov¹, M.A. Putyato¹, V.V. Preobrazhenskii¹, T.B. Popova²,
V.I. Ushanov², V.V. Chaldyshev²

¹ Rzhanov Institute of Semiconductor Physics, Siberian Branch, Russian Academy of Sciences,
630090 Novosibirsk, Russia

² Ioffe Institute,
194021 St. Petersburg, Russia

E-mail: chald.gvg@mail.ioffe.ru

Received November 8, 2021

Revised November 12, 2021

Accepted November 12, 2021

By molecular-beam epitaxy we have grown epitaxial layers of GaAs_{1-x}Bi_x solid solutions with a bismuth content of $0 < x < 0.02$. Structural and optical properties of the layers were investigated. We determine the influence of the bismuth flux and substrate temperature on the bismuth incorporation into the growing layers.

Keywords: gallium arsenide, bismuth, molecular-beam epitaxy, bandgap.

DOI: 10.21883/SC.2022.03.53057.9764

1. Introduction

Bismuth is a V group substitutional isovalent impurity that forms solid solutions with III–V compounds [1]. However, equilibrium solubility of bismuth in gallium arsenide at temperatures typical for epitaxial growth of this material is low and does not allow to significantly change the bandgap width for epitaxial layer grown under conditions for example, when using a liquid-phase epitaxy method [2,3]. Nevertheless, bismuth doping has a strong influence on the electrophysical properties of the grown layers (see [4–7] and literature review in [1]).

A significant (up to 3.1%) bismuth concentration x in GaAs_{1-x}Bi_x solid solution was achieved in 2003, using a molecular beam epitaxy (MBE) method at low growth temperature [8]. Diluted GaAs_{1-x}Bi_x solid solutions were found to demonstrate significant reduction of the bandgap width E_g even with low the rather bismuth concentration x [9]. Thus, bismuthides expand the heterostructure development capabilities in III–V materials system and, therefore, offer opportunities for the development and application of new heterostructures.

Since GaAs_{1-x}Bi_x is grown using MBE method at low temperature (LT), the applications of this material primarily involve on the base of LT-GaAs devices developed earlier. The most important of them include ultra high-speed photodetectors, generators and receivers of terahertz radiation. Reduction of the bandgap width by bismuth doping of GaAs was found to extend the spectral sensitivity range of optoelectronic devices up to 1.3 μm and farther, which corresponds to O-band of fiber-optic communication [10]. In addition, modification of the band structure makes it possible to reduce the excessive noise from avalanche diodes [11] and considerably improve performance of terahertz frequency band devices [12].

Currently, the LT-GaAs_{1-x}Bi_x epitaxial layer formation process using MBE method is only being developed as

evidenced by a large number of publications addressing both epitaxial growth models and specific epitaxial process modes and conditions [13–19].

In this paper we study the influence of the growth temperature and the bismuth and arsenic vapor pressure on the structure and optical properties of GaAs layers grown using MBE method.

2. Epitaxial layer growth

The test samples were grown on semi-insulating GaAs substrates using the MBE method. The processes on the growth surface were controlled using a reflection high-energy electron diffraction (RHEED) method. Molecular flux density was measured using a vacuum ionization gauge that was inserted in the growth region for the measurement period.

The substrate temperature was measured using a calibrated thermocouple attached to the manipulator heater. The thermocouple was calibrated according to the transition temperatures of gallium arsenide surface structures.

In the first set of experiments we studied the influence of the bismuth flux rate on the Bi incorporation into the GaAs growing layer and surface morphology.

After removal of the protective oxide layer, a 0.2 μm GaAs buffer layer was grown on the substrate surface at the rate of 1 $\mu\text{m}/\text{h}$. Growth took place at a temperature of 580°C under the conditions of the surface reconstruction (2 \times 4). Then the growth was interrupted, the substrate temperature was reduced down to 380°C, growth rate was reduced down to 0.3 monolayer per second (ML/s). The growth took place under the conditions of coexistence of surface reconstructions ((2)(3) \times (4)(6)). This provided the growth under near-stoichiometric conditions. Bi flow was equal to $5 \cdot 10^{-9}$, $1 \cdot 10^{-8}$, $2 \cdot 10^{-8}$, $4 \cdot 10^{-8}$ Torr. The thickness of grown epitaxial layers was equal to 0.3 μm .

Parameters of GaAs_{1-x}Bi_x samples (growth temperature, Bi molecular concentration, diffraction curve width, optical absorption edge displacement relative to the reference sample BP2970)

Sample	$T_{\text{growth}}, ^\circ\text{C}$	x , mol% (EPMA)	x , mol% (HRXD)	FWHM $\mathbf{g} = [004]$, arcseconds	ΔE , eV
BP2978	150	1.6	2.0	64	-0.245
BP2977	200	1.8	1.9	62	-0.138
BP2976	250	1.6	1.6	65	-0.103
BP2975	300	1.6	1.4	73	-0.089
BP2979	340	1.0			-0.068
BP2974	340	1.4			-0.076
BP2970	380	0.0			0.000

For growth with maximum bismuth flow, transition $((2)(3) \times (4)(6)) \rightarrow (2 \times 1)$ is observed rather quickly. For growth with $P_{\text{Bi}} = 2 \cdot 10^{-8}$, $1 \cdot 10^{-8}$, $5 \cdot 10^{-9}$ Torr, the interval of time from the beginning of growth to the superstructure superposition transition $((2)(3) \times (4)(6)) \rightarrow (2 \times 4(1))$ depends on the Bi flow rate — the lower the flow is, the higher the interval is. This is probably due to Bi segregation and accumulation on the growth surface. Surface morphology observed visually in the reflected light varied from mirror-smooth for minimum P_{Bi} to opaque for maximum P_{Bi} .

In the second set of experiments we studied the influence of the growth temperature on Bi incorporation into the growing epitaxial GaAs layer and surface morphology after growth.

A set of samples was grown with $P_{\text{Bi}} = 2 \cdot 10^{-8}$ Torr. The growth temperatures were $T_s = 440$ (BP2973), 380 (BP2972), 340 (BP2974), 300 (BP2975), 250 (BP2976), 200 (BP2977), 150°C (BP2978). During growth in the range from 440 to 340°C surface superstructure transition $((2)(3) \times (4)(6)) \rightarrow (2 \times 4(1))$ was observed. Bi segregation in this temperature range resulted in Bi accumulation on the surface which ensured occurrence of profile observed visually in a form of a „mat“ in reflected light. Additionally, BP2970 reference sample was grown at 380°C with low pressure of Bi vapor ($5 \cdot 10^{-9}$ Torr).

For samples growing at 300 and 250°C, reconstruction transition $((3 \times 1) \rightarrow (1 \times 3))$ was observed with the reconstruction remaining unchanged throughout the growth process. Sample growth at 200 and 150°C took place without reconstruction. Only main reflection strands were observed.

Such form of diffraction pattern is specific to GaAs growing at low temperatures. Mirror-smooth surface for samples grown at 300°C and lower temperature is likely associated with reduction or probably with suppression of Bi segregation.

A sample was grown at 200°C and $P_{\text{Bi}} = 4 \cdot 10^{-8}$ Torr. Growth took place without a reconstruction of the surface. The surface after growth is mirror-smooth that can also be indicative of significantly reduced Bi segregation.

3. Structure and composition investigations

The film composition was determined by an electron probe microanalysis (EPMA) using Camebax (France) microanalyzer equipped with four X-ray spectrometers. The composition was analyzed at accelerating electron voltage 10 keV and specimen current 10 nA. A stoichiometric GaAs sample and metallic Bi were used as reference standards. Ga: L_{α} , As: L_{α} and Bi: M_{α} were used as analytical lines.

In the samples grown at 380°C, bismuth concentration was lower than the method's detection limit ($x < 0.8$ mole%) for any bismuth fluxes used in our experiments. Bismuth was found in the samples from the second set grown at a lower temperature. The measurement error was ± 0.2 mole%. The measurement results are shown in the table.

For structural characterization of samples, a high-resolution X-ray diffraction (HRXD) method was used. Diffraction reflection curves (DRC) were obtained using a low-dispersion double-crystal version of reflection-type imaging, geometry $(+n, -m)$, $\text{CuK}\alpha_1$ -emission. Ge single crystal with orientation (001) was used as a monochromator. Reflection from the monochromator $\mathbf{g} = [004]$. DRCs were recorded in reflections from the sample for $\mathbf{g} = [004]$ and $\mathbf{g} = [224]$. In the last case, grazing incidence angle geometry and grazing reflection angle geometry were used.

Reflection $\mathbf{g} = [004]$ was used to measure the full width at half maximum (FWHM) of the film peaks. The distance between the thickness oscillations was used to check the GaAs_{1-x}Bi_x layer thickness. A DRC pair $\mathbf{g} = [224]$ was used to calculate the layer strain state within a tetragonal model[20]. For the calculation, the GaAs_{1-x}Bi_x solid solution was considered and $a_{\text{GaAs}} = 0.5653$ and $a_{\text{GaBi}} = 0.6324$ nm lattice parameters were used.

Figure 1 shows DRCs of four GaAs_{1-x}Bi_x samples obtained in the vicinity of reflection $\mathbf{g} = [004]$. Angular position of the substrate diffraction peak was assumed as the reference. For better perception, they are vertically displaced from each other with $\times 10$. Only film and

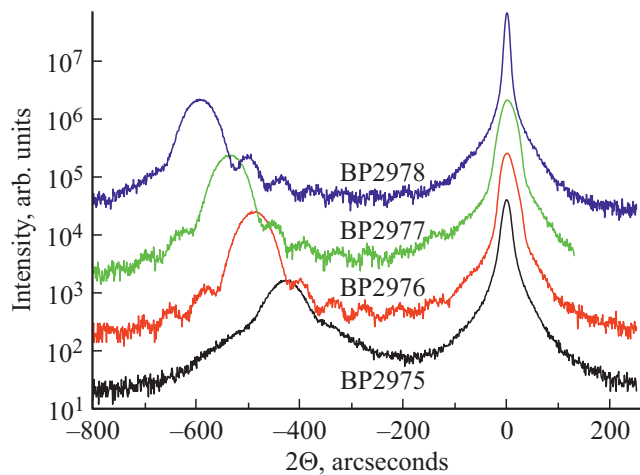


Figure 1. Diffraction reflection curves in the vicinity of reflection $g = [004]$ for GaAs_{1-x}Bi_x samples.

substrate peaks are visible on DRCs of BP2975 sample. FWHM of film peak is equal to 73 arcseconds. A significant broadening is observed on the bottom of DRC. Since MBE ensures high horizontal homogeneity of grown layers, this widening is indicative of deformation heterogeneity through the GaAs_{1-x}Bi_x layer thickness. The most probable cause of this heterogeneity is the bismuth concentration gradient through the film thickness. Presence of such gradient also proves the absence of thickness oscillations.

For BP2976, BP2977 and BP2978 samples, in addition to the film and substrate peaks, thickness oscillation peaks are also present on DRCs. FWHMs of film-related peaks are equal to 65, 62 and 64 arcseconds, respectively. Such recorded oscillations on the rocking curve are indicative of the GaAs_{1-x}Bi_x layer homogeneity and sharp boundaries. Thickness oscillation period is ~ 60 arcseconds that is equal to a GaAs_{1-x}Bi_x layer thickness $d \approx 300$ nm.

The calculated Bi concentrations in the layers are shown in the table. It can be seen that EPMA and HRXD data are matched quantitatively.

4. Optical investigations

Optical characteristics of samples were studied using light reflection, transmission and extinction spectroscopy at normal incidence within the wavelength range of 900–1600 nm at room temperature. Osram HLX 100W 6.6A with a collimator was used as an emission source. The spectra were recorded using OceanOptics NIRQuest-512 spectrometer. The spectra were recorded using OceanOptics SpectraSuite software.

Figure 2 shows the optical extinction spectra of samples grown at constant Bi flow at $P_{\text{Bi}} = 2 \cdot 10^{-8}$ Torr within the growth temperature range of 150–440°C. The spectra were obtained from the measured transmittance spectra using the

Bouguer-Lambert-Beer law

$$\alpha = -\ln(T_\alpha/T_0)/d, \quad (1)$$

where d is the thickness of the epitaxial film of interest, T_α is the optical transmittance spectrum of the film, and T_0 is the reference transmittance spectrum of Bi-free GaAs grown under standard conditions.

The figure shows that wide absorption tails extending up to 1500 nm wavelength are formed in optical spectra with reduction of the growth temperature. Such features of optical extinction in non-stoichiometric epitaxial GaAs films are well known [21] and are due to light absorption and dispersion in disordered systems of As_{Ga} point antisite defects within the film [22–24]. In addition, the optical absorption coefficient is increased significantly with reduction of growth temperature as a result of increase in the concentration of non-stoichiometric As [22–24] and reaches $2 \cdot 10^4 \text{ cm}^{-1}$ for BP2978 sample grown at 150°C.

In addition, with the growth temperature variation, optical absorption edge displacement is observed that is probably due to the impact of the Bi atom concentration growth on the bandgap of LT-GaAs_{1-x}Bi_x material. Qualitative assessment of the optical absorption displacement was carried out by means of a linear interpolation of a spectral region within 900–1000 nm relative to BP2970 reference sample. A sample grown at minimum temperature 150°C was not considered due to significant influence of high

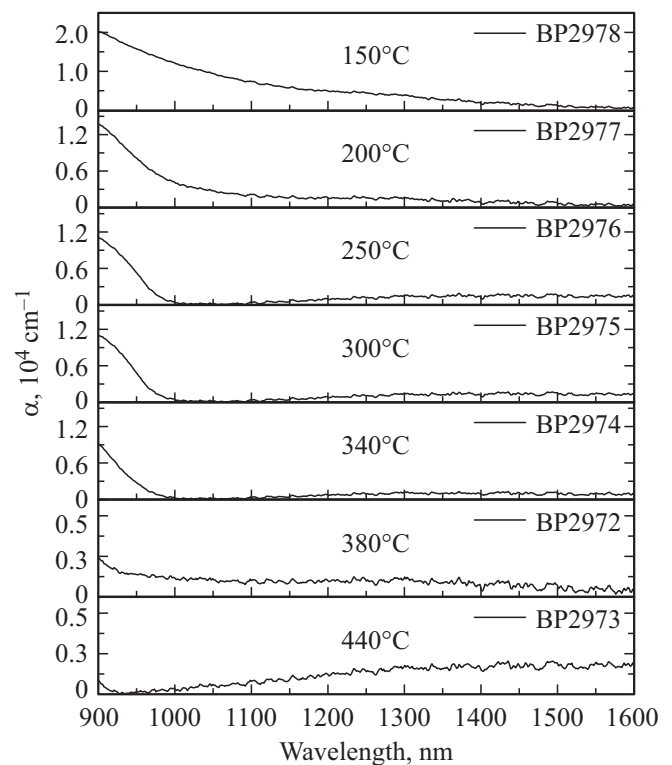


Figure 2. Optical extinction coefficient spectra of GaAs_{1-x}Bi_x samples vs. the growth temperature at constant pressure of Bi vapors $P_{\text{Bi}} = 2 \cdot 10^{-8}$ Torr.

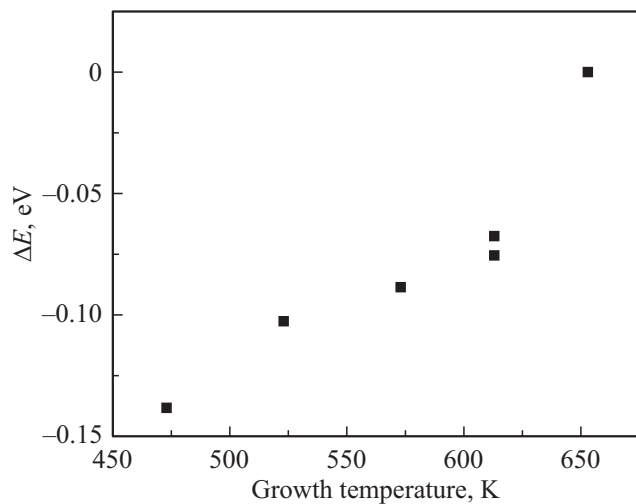


Figure 3. Optical absorption edge displacement depending on the sample growth temperature.

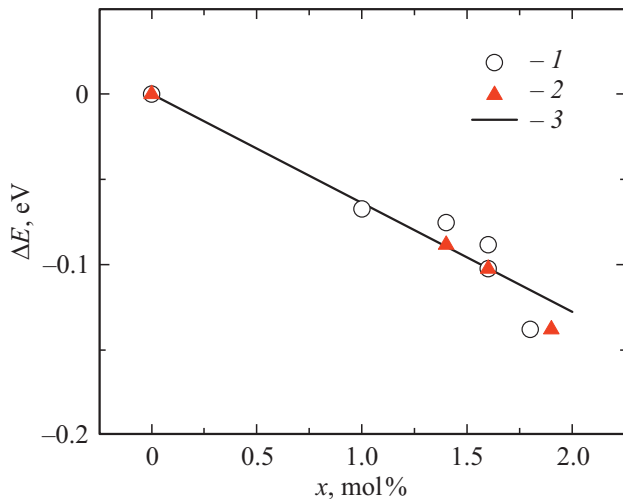


Figure 4. Optical absorption edge displacement of $\text{GaAs}_{1-x}\text{Bi}_x$ depending on the molecular concentration of Bi measured using EPMA (1) and HXRD (2) methods. Solid line (3) shows a linear approximation from [25].

concentration of excessive As atoms on the visible spectrum shape [22–24]. The results are shown in Fig. 3.

The absolute optical absorption edge displacement is increased with decrease of the sample growth temperature. This fact suggests that Bi concentration in epitaxial films is increased at constant pressure of Bi vapors with decrease in the growth temperature. In particular, this is supported by the measurements of Bi molecular concentration using EPMA and HXRD methods (see the table).

The corresponding relationships of the optical absorption edge displacement vs. the measured molecular concentrations of Bi using EPMA and HXRD methods are shown in Fig. 4. A sample grown at minimum temperature 150°C was not considered due to significant influence of high

concentration of excessive As atoms on the visible spectrum shape [22–24].

A solid black line shows a linear fitting relationship of the bandgap width variation of $\text{GaAs}_{1-x}\text{Bi}_x$ material vs. Bi concentration ($\Delta E = -6.4x$) obtained in [25]. As can be seen, this approximation quantitatively describes the measured relationship.

5. Discussion of results

The investigations have shown that due to Bi atom segregation and competition with As atoms during incorporation into a growing crystal, growth of $\text{GaAs}_{1-x}\text{Bi}_x$ layers may only take place in a narrow growth conditions range: temperature should be below 350°C and ratio of (As + Bi) and Ga on the growing surface should be stoichiometric, i.e. near the boundary of morphological stability. Intersection of this boundary is followed by a sharp increase in the roughness of the growing $\text{GaAs}_{1-x}\text{Bi}_x$ layer and by formation of Bi and Ga drops and then by formation of metal inclusions. In additions, the layer surface morphology may be affected by stresses and dislocations since the lattice parameters differ for the $\text{GaAs}_{1-x}\text{Bi}_x$ layer and GaAs substrate. Therefore, there should be an effective continuous monitoring of the $\text{GaAs}_{1-x}\text{Bi}_x$ layer surface during the growth (*in situ*).

Composition homogeneity of the $\text{GaAs}_{1-x}\text{Bi}_x$ layers to be grown is ensured at epitaxy temperatures of $150\text{--}250^\circ\text{C}$, but at higher temperatures, bismuth segregation leads to composition gradient through the thickness. At an extreme low growth temperature of 150°C , large amount of excess arsenic atoms are captured in the growing layer by formation of antisite defects. MBE technology at low temperature with precise control of molecular flux ratio made it possible to form $\text{GaAs}_{1-x}\text{Bi}_x$ layers with bismuth concentration x up to 2 mole%.

Optical investigations have proved that a relatively low bismuth concentration leads to rather considerable restriction of the material bandgap. Taking into account the influence of band tails caused by the formation of antisite defects in arsenic, bandgap width variation due to formation of a $\text{GaAs}_{1-x}\text{Bi}_x$ solid solution may be described by linear law $\Delta E = -6.4x$ that was established experimentally in [25]. The achieved maximum reduction of the bandgap associated with formation of $\text{GaAs}_{1-x}\text{Bi}_x$ solid solution is $\sim 0.14\text{ eV}$ with a bismuth concentration of $\sim 2\text{ mole\%}$ and takes place at an epitaxy temperature of 200°C .

6. Conclusion

MBE method at a low temperature of $150\text{--}350^\circ\text{C}$ has been used to grow epitaxial layers of $0.3\ \mu\text{m}$ $\text{GaAs}_{1-x}\text{Bi}_x$ solid solutions with bismuth concentration $0 < x < 0.02$. At higher growth temperatures, bismuth capture into the growing layer is inefficient at any molecular flow ratio. The relationship of bismuth concentration in the grown layers vs.

temperature has been determined experimentally. Structural and optical properties of the layers have been studied. The epitaxial layers have been shown to have rather high crystalline perfection. It was observed that the formation of GaAs_{1-x}Bi_x solid solution leads to linear reduction of the bandgap width. The bandgap reduction by 0.14 eV was achieved at bismuth concentration of ~ 2 mole%. Such bandgap variation takes place in a sample grown at an epitaxy temperature of 200°C and $P_{\text{Bi}} = 2 \cdot 10^{-8}$ Torr.

Conflict of interests

The authors declare that they have no conflict of interest.

References

- [1] V.V. Chaldyshev, S.V. Novikov. *Isovalent impurity doping of direct-gap III-V semiconductor layers*. In: *Semiconductor Technology: Processing and Novel Fabrication Techniques*, eds. M. Levinshtein and M. Shur (Wiley-Interscience, N.Y., USA, 1997).
- [2] R.Kh. Akchurin, Yu.F. Biryulin, Le Din Cao, V.I. Fistul, V.V. Chaldyshev. *Elektron. tekhn. Materialy*, **11**, 22 (1984) (in Russian).
- [3] Yu.F. Biryulin, N.V. Ganina, V.V. Chaldyshev, Yu.V. Shmartsev. *FTP*, **19**(6), 1104 (1985) (in Russian).
- [4] N.V. Ganina, V.B. Ufimtsev, V.I. Fistul. *Pis'ma ZhTF*, **8**, 620 (1982) (in Russian).
- [5] Yu.F. Biryulin, N.V. Ganina, V.V. Chaldyshev, Yu.V. Shmartsev. *Pis'ma ZhTF*, **12**(5), 274 (1986) (in Russian).
- [6] Yu.F. Biryulin, L.V. Golubev, S.V. Novikov, V.V. Chaldyshev, Yu.V. Shmartsev. *FTP*, **21**(5), 949 (1987) (in Russian).
- [7] Yu.F. Biryulin, V.V. Vorobieva, V.G. Golubev, L.V. Golubev, V.I. Ivanov-Omsky, S.V. Novikov, A.V. Osutin, I.G. Saveliev, V.V. Chaldyshev, Yu.V. Shmartsev, O.V. Yaroshevich. *FTP*, **21**(12), 2201 (1987) (in Russian).
- [8] S. Tixier, M. Adamcyk, T. Tiedje, S. Francoeur, A. Mascarenhas, P. Wei, F. Schiettekatte. *Appl. Phys. Lett.*, **82**(14), 2245 (2003).
- [9] S. Francoeur, M.-J. Seong, A. Mascarenhas, S. Tixier, M. Adamcyk, T. Tiedje. *Appl. Phys. Lett.*, **82**(22), 3874 (2003).
- [10] E. Tisbi, E. Placidi, R. Magri, P. Proposito, R. Francini, A. Zaganelli, S. Cecchi, E. Zallo, R. Calarco, E. Luna, J. Honolka, M. Vondráček, S. Colonna, F. Arciprete. *Phys. Rev. Appl.*, **14**(1), 014028 (2020).
- [11] Yuchen Liu, Xin Yi, N.J. Bailey, Zhize Zhou, T.B.O. Rockett, Leh W. Lim, Chee H. Tan, R.D. Richards, J.P.R. David. *Nature Commun.*, **12**(1), 4784 (2021).
- [12] K. Bertulis, A. Krotkus, G. Aleksejenko, V. Pačebutas, R. Adomavičius, G. Molis, S. Marcinkevičius. *Appl. Phys. Lett.*, **88**(20), 201112 (2006).
- [13] Sonia Blel, C. Bilel. *J. Electron. Mater.*, **50**(6), 3380 (2021).
- [14] S.T. Schaefer, M.S. Milosavljevic, R.R. Kosireddy, S.R. Johnson. *J. Appl. Phys.*, **129**(3), 035303 (2021).
- [15] Y. Guan, G. Luo, D. Morgan, S.E. Babcock, T.F. Kuech. *J. Phys. Chem. Solids*, **138**, 109245 (2020).
- [16] M.A. Stevens, K.A. Grossklaus, T.E. Vandervelde. *J. Cryst. Growth*, **527**, 125216 (2019).
- [17] C. Cornille, A. Arnoult, Q. Gravelier, C. Fontaine. *J. Appl. Phys.*, **126**(9), 093106 (2019).
- [18] M.A. Stevens, K.A. Grossklaus, J.H. McElearney, T.E. Vandervelde. *J. Electron. Mater.*, **48**(5), 3376 (2019).
- [19] J. Puustinen, J. Hilska, M. Guina. *J. Cryst. Growth*, **511**, 33 (2019).
- [20] P. van der Sluis. *J. Phys. D: Appl. Phys.*, **26**, A188 (1993).
- [21] G.M. Martin. *Appl. Phys. Lett.*, **39**, 9 (1981).
- [22] L.G. Lavrent'eva, M.D. Vilisova, V.V. Preobrazhenskii, V.V. Chaldyshev. *Crystallography Reports*, **47**, S118 (2002).
- [23] V.V. Chaldyshev. *Mater. Sci. Eng. B*, **88**, 195 (2002).
- [24] M.R. Melloch, J.M. Woodall, E.S. Harmon, N. Otsuka, F.H. Pollak, D.D. Nolte, R.M. Feenstra, M.A. Lutz. *Annual Rev. Mater. Sci.*, **25**, 547 (1995).
- [25] A.R. Mohmad, F. Bastiman, J.S. Ng, S.J. Sweeney, J.P.R. David. *Phys. Status Solidi C*, **9**(2), 259 (2012).